

## DISC IMAGE-PROCESSING SOFTWARE FOR THREE-DIMENSIONAL MAPPING OF STEM RING WIDTH AND COMPRESSION WOOD

DAVID PONT\*, ROD K. BROWNLIE, and JENNIFER C. GRACE

Ensis, Private Bag 3020, Rotorua, New Zealand.

(Received for publication 7 November 2006; revision 21 March 2007)

### ABSTRACT

New tools have been developed to map the three-dimensional variation of wood properties within tree stems in order to support research into modelling tree growth and stem wood properties. Digital imaging, image processing, and data visualisation techniques have been integrated into software tools (G2Ring and G2View) that allow cost-effective three-dimensional stem analysis.

Specialised image-processing algorithms have been developed to accurately delineate annual ring boundaries and sectors of compression wood on images of cross-cut discs. Discs are cut by chainsaw, wetted to improve contrast, and imaged in the field. The image-processing algorithms handle the significant image “noise” resulting from the surface roughness of the discs. Annual ring detection is sufficiently robust that localised surface markings or defects (such as knots and cracks) do not substantially affect accuracy and the algorithm for detection of compression wood addresses the problem of false classification of latewood. The software, developed on images of discs from *Pinus radiata* D. Don, uses an efficient combination of automatic detection with operator guidance and override to maximise accuracy and efficiency.

The software incorporates a facility to reconstruct three-dimensional stem models by assembling data from multiple spatially registered discs. Optional information on three-dimensional stem shape, obtained from the existing image-based PhotoMARVL system, allows inclusion of stem sinuosity in the three-dimensional stem model. Custom visualisation software (G2View) has been developed to examine the three-dimensional distribution of measured data, such as ring width and compression wood, within the stem. Visualisation of the stem analysis data is a useful analytical precursor to modelling stem structure.

PhotoMARVL, G2Ring, and G2View thus provide a set of tools, able to be used individually and in combination, to collect data useful for analysis and modelling of stem shape and internal structure.

---

\* Corresponding author: david.pont@ensisjv.com

**Keywords:** image-processing; disc; ring width; compression wood; *Pinus radiata*.

## INTRODUCTION

The suitability of a tree for a particular end use depends largely on the properties of the wood within the stem. General patterns of variation in key wood properties for New Zealand *Pinus radiata* are understood in relation to height within the stem and ring number from the pith (Harris & Cown 1991), but significant variation in properties occurs between individual trees in forest stands. In addition stem sinuosity, out-of-round (OOR) cross section, pith eccentricity, and compression wood (CW) are well-known features associated with variability in wood properties within individual trees.

Variability between and within trees is an important issue for utilisation of forest products, causing inefficient resource allocation and poor product performance. It would be useful to predict properties and variability within trees and logs from readily observable characteristics in order to make better decisions in operations such as stand selection, log making, log grading, and sawing. In order to carry out research into within-stem variation in wood properties a data collection system was developed. The system consists of three components: an existing tool to capture stem shape (PhotoMARVL, Firth *et al.* 2000); a new tool to digitise annual rings and compression wood on discs; a new tool to construct and visualise a three-dimensional model of a stem and its properties. In this paper the relevant literature is reviewed and then the development of the new tools is described.

## Literature Review

### *Stem analysis*

Classical stem analysis has been used for the retrospective study of stem growth, usually in terms of volume, basal area, and taper (Duff & Nolan 1953, 1957; Assmann 1970; Husch *et al.* 2003) by measurement of annual ring radii on discs cut at mid-internode along the stem. Stem analysis provides essential quantitative data but lacks information about stem quality. To assess key determinants of stem quality studies have been made of the relationships between stem shape, lean, pith eccentricity, out-of-round, and compression wood by, for example, Burdon (1975), Nicholls (1982), Alteyrac *et al.* (1999), Saint-Andre & Leban (2000), Constant *et al.* (2003), Warensjö *et al.* (2004), and Duncker & Warensjö (2005). Harris (1976) noted that compression wood, especially when severe, reduced strength and stability in timber, while high lignin content and other adverse properties made it undesirable for pulping. Nicholls (1982), in discussion of utilisation issues associated with stem shape and compression wood, identified a number of negative impacts on the qualities of sawn timber, veneer, and pulp. Burdon (1975) pointed out that compression wood is normally assumed to be formed in response to deviations

from verticality, but showed that different clones vary in their propensity to form compression wood.

#### *Growth ring measurement*

Biging & Wensel (1984) developed a method for counting and measuring rings on photographic transparencies of discs, finding the method gave accuracy similar to measuring the discs directly and without bias. Significant benefits identified were the reduced time in the field, no need to transfer large numbers of discs to the laboratory, avoidance of problems with shrinkage and degradation of discs, and a permanent photographic record for future reference.

Currently there are a number of image-based systems for measuring radii — for example, WinDENDRO (WinDENDRO 2004) is a widely used commercial system. Many of these systems utilise image-processing techniques to locate ring boundaries along a radial direction on a disc image — for example, MacDENDRO (Guay *et al.* 1992), WinDENDRO (WinDENDRO 2004), Connor (1999), and Biging & Wensel (1984) — with the option of making measurements on additional radii. Such systems use edge detection methods in an essentially one-dimensional domain.

As noted by Yanosky & Robinove (1986) and Soille & Misson (2001), estimates of ring area based on a few (two, four, or eight) radii can give significant errors. Yanosky & Robinove (1986) used direct manual digitisation on a disc image to outline annular regions and briefly analysed the benefits of increasing numbers of radii on ring area estimates; Soille & Misson (2001) used morphological operations on disc images to delineate annual rings. These are examples of systems that operate in the two-dimensional domain, generating a continuous boundary enclosing an annual ring on the disc image. Accuracy of ring area measurement in a two-dimensional system is determined by accuracy of the boundary placement and resolution of the image. Even with relatively low-resolution images, the effective number of radii measured is generally much higher than the numbers practical with a one-dimensional system. Edge detection in a one-dimensional system is sensitive to errors resulting from the processing of a narrow (nominally one pixel wide) sector of an annual ring, where local features including noise, false or faint rings, knots, and other imperfections strongly determine the result. These problems can be reduced in a two-dimensional system at a cost of increased processing complexity and time.

#### *Compression wood measurement*

Timell (1986) gave thorough treatment to the appearance, features, and causes of compression wood, and Duncker & Warensjö (2005) also produced a useful review of the topic. It is generally accepted that compression wood is visibly darker in

appearance than normal wood (Pillow 1941; Timell 1986). This altered appearance is attributed to greater light absorption due to higher lignin content, and lower light-scattering due to thicker cell walls (Duncker & Warensjö 2005). Various researchers, including Pillow (1941), Nicholls (1982), and Timell (1986), have described a darker appearance of wood with more severe compression wood, while in some studies the amount of the annual ring with compression wood was also classified as more severe (Burdon 1975; Harris 1976). These criteria have been used to classify regions of compression wood into one of a number of grades. The use of transmitted light through thin sections (2–3 mm) is an often-used method of accurately classifying compression wood but this method has the drawback of onerous disc preparation. Timell (1986) noted that wetting refreshes the “green” appearance of wood, improving the contrast between different grades of compression wood and normal wood, especially in conifers.

As with annual rings, the measurement of compression wood on disc surfaces is now carried out largely using image-processing techniques, replacing earlier techniques such as use of a planimeter or counting dots on a grid overlay. Examples of image-processing techniques have been provided by Andersson & Walter (1995) who used supervised maximum-likelihood classification, Nyström & Kline (2000) who used a multivariate regression model, and Wernsdörfer *et al.* (2004) who used the Magic Wand tool in Photoshop (a popular image-editing tool). These methods are based on the same principle: classification of image pixels with similar appearance to that indicated by an operator. One common problem with using image-processing to classify compression wood is the false classification of latewood (LW). This issue was noted by Andersson & Walter (1995) and Nyström & Kline (2000) and is due to the similarity in appearance of the two types of wood and the fact that compression wood often occurs in the latewood portion of an annual ring.

### *Stem visualisation*

There are many methods for presenting images and data relating to a two-dimensional surface such as a disc cut from a tree. Increasingly, more-advanced scientific visualisation techniques are required for examining three-dimensional domains such as reconstruction of a tree stem from an axial series of two-dimensional slices. A number of software tools, developed for applications such as medical imaging and engineering, utilise the graphics capabilities of current desktop and laptop computers to view three-dimensional data. One such tool is the VTK software library (Schroeder *et al.* 2004) that enables the development of general purpose and custom-built visualisation software.

In summary, the importance to end-users of variability in wood properties has driven current wood quality research to examine relationships between stem

geometry and wood properties in greater detail. The first step in understanding the three-dimensional variation of wood properties within stems is to be able to measure and map stem structure. Computer-based methods offer a cost-effective means of providing the tools required to support this research.

## MATERIALS

This paper outlines recently developed tools for reconstruction of three-dimensional stem structure incorporating stem shape, annual rings, and the location of compression wood. These tools are illustrated using data from a *P. radiata* tree (Tree 121) with a sinuous stem growing in an experimental block in the central North Island of New Zealand. Twenty-one discs were cut at mid-internode positions in the lower two-thirds of the stem of Tree 121, at heights ranging from 0.47 to 17.10 m. Ring counts ranged from 19 in the lowest three discs to 13 in the uppermost six discs.

## METHODS

### Standing Tree Measurement and Disc Extraction

The tree was photographed and measured according to the method described by Firth *et al.* (2000) to provide three-dimensional stem shape. A compass bearing (*B1*), from the camera position to the centre of the tree, was recorded. A vertical reference line was marked on the stem from ground level to 2 m. After the tree was felled, the reference line was extended along the full length of the stem and the compass bearing (*B2*) from the centre of the stump to the reference line on the edge of the stump was recorded. Stump height was recorded, disc positions were marked in the middle of each internode, and their distances from the base of the felled stem were recorded. Discs 50 mm in thickness were cut with a chainsaw, and then labelled with a tag attached to the bark.

### Image Capture

The freshly cut discs were mounted on a reference frame and photographed with a hand-held digital camera. The frame contained five pins — one at the centre and one in each corner of a 500-mm square (*see* Fig. 1) — and was used to provide control points for image correction and scaling. The pins were 5 mm in diameter and extended 50 mm above the surface of the board to establish a measurement plane coincident with the top surface of the discs (nominally 50 mm thick). A 5-mm hole was drilled in the centre of the pith of each disc to locate it on the centre pin. The disc was then washed with water to remove surface contamination and enhance contrast of the annual rings and any compression wood, located on the centre pin, and rotated so that the reference line marked in the field aligned with the vertical line at the top of the frame.



FIG. 1—Image of sample disc 121/17 on the reference frame. Four pins extending 50 mm above the frame surface were located at the corners of a square of known dimension (500 mm) to establish a measurement plane.



FIG. 2—Image of sample disc 121/17 corrected for perspective distortion using a two-dimensional projective transform.

### Image Pre-processing

All image-processing to digitise annual rings and compression wood on disc images described in this paper was carried out using a purpose-built software program named G2Ring. The image-processing algorithms in G2Ring are outlined here, and values for image-processing parameters follow in the Results section. Initially the centres of the top ends of the four corner pins (*A*, *B*, *C*, and *D* clockwise from the top left corner) were digitised on the disc image and the known co-ordinates of these four control points were used to apply a two-dimensional projective transform (Wolf 1983) to obtain an image free from perspective distortion and rotation due to camera orientation (*see* Fig. 2). The correction required here was small but this procedure ensures accuracy from images taken with a hand-held camera. The resulting corrected images were approximately 1200 by 1200 pixels (dependent on the size of the frame in the original image). The centre of the pith was digitised to establish the origin (*O*) of the disc measurement system. The corrected image was mapped from polar (Fig. 2) to rectangular co-ordinates (Fig. 3) to speed up image-processing by avoiding repeated use of trigonometric functions.

The chainsaw-cut disc surfaces were very rough in comparison with those in typical disc image-processing applications, resulting in a lot of image “noise”. Median filtering removed a large amount of this noise while preserving edges, notably the annual ring boundaries. The median filtering and mapping were integrated into a

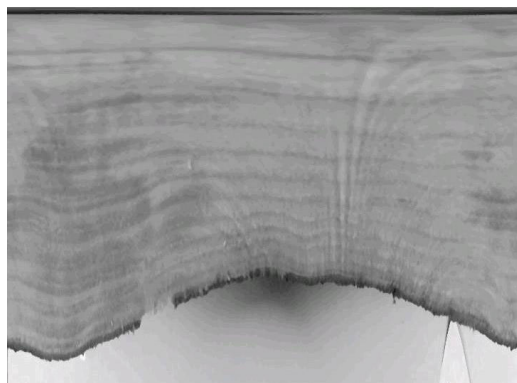


FIG. 3—Output image from the re-mapping and smoothing process. The pith is stretched along the top of the image and the bark is at the base of the image.

single process, sampling the corrected image with a window of size  $2rr+1$  and  $2rt+1$  pixels in the radial and tangential directions respectively. Sampling was carried out on a regular grid in polar coordinates using  $R$  angular steps and  $S$  radial steps of size one pixel from  $O$  outwards to the edge of the image. The median value of pixels within the window at each angular ( $r$ ) and radial ( $s$ ) step was used to assemble a rectangular output image of width  $R$  and height  $S$  (note that  $S = \text{distance } OA$ ).

Enhancement of edges was carried out using a gradient-based filter with a window of size  $et$  by  $er$  pixels in the tangential and radial directions respectively. After initial testing  $et=1$  was found to be satisfactory, limiting the filter to the radial direction, across ring boundaries. For each pixel in the re-mapped and smoothed image, the difference in grayscale value compared with each pixel in the window was evaluated. The difference values were encoded using a vector dot product, based on treatment of the grayscale image as a terrain where grayscale values equate to elevations above the regular grid of pixel locations. Grayscale values for two pixels were used to define a vector, and evaluating the dot product of this vector with a vertical unit vector produced values ranging from  $-1$  to  $1$  where  $0$  represents zero gradient, and positive and negative values represent regions of increasing or decreasing grayscale values respectively. The median of all values within the window was taken. As a final step the values mapped linearly into the range  $0-255$  to allow convenient storage and viewing of the output as a grayscale image.

### Tree Ring Delineation

Edge detection was carried out by evaluating the mean grayscale value on the edge-enhanced image for all pixels lying under a curve extending from the left-hand to right-hand sides of the edge-enhanced image from the previous step (*see* Fig. 4). Due to the continuity of the re-mapped images at the left-hand and right-hand sides, this curve was equivalent to a closed loop on the original image. The location and shape of the curve were adjusted to maximise the mean value under the line, given

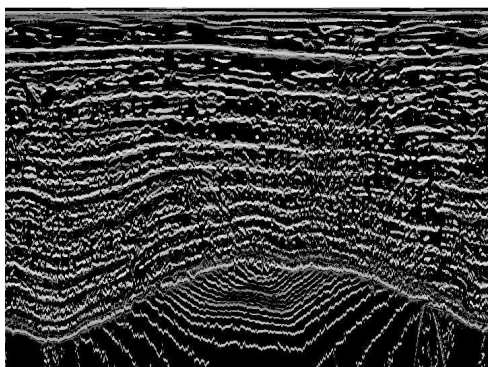


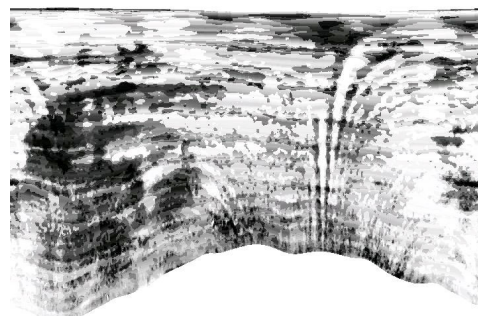
FIG. 4—Output image from the filter used for edge enhancement. Regions of positive gradient such as the latewood/earlywood transition are coloured white.

that high positive gradient values will occur in the latewood to earlywood transition. Adjustment of the line used a multi-scale approach by moving segments of the line to the location of the local maximum within a neighbourhood that reduced in size at each successive scale. At each scale all sub-segments of the curve of width  $ws$  were evaluated at  $rl$  positions above and below (in a radial direction) the current position and if a higher value than that at the current location was found the curve segment was moved to the new location. The process was fixed to occur in 10 steps with a linear reduction of  $ws$  and  $rl$  at each step to a value of 1 for both in the final step.

### Compression Wood Mapping

Given a disc image with annual ring boundaries delineated (by the process described above), compression wood was identified by comparing grayscale values in the tangential direction around each annual ring. The process was carried out using the re-mapped and smoothed image produced earlier (Fig. 3). Two consecutive annual ring boundaries delimit an annual ring, with maximum ring width  $rw$  (pixels). The annual ring was divided in the radial direction into  $rw$  equally spaced bands (of one pixel width in the radial direction). A histogram of grayscale values in each band was used to generate a new image ( $Ir$ ) containing pixel values equalised across the range observed for the band, enhancing contrast and the appearance of any compression wood (Fig. 5). Pixels were classified as compression wood (relatively dark on the equalised image) using a threshold value  $T$  applied on the image  $Ir$ . Based on the understanding that more severe compression wood is darker and occupies a greater portion of the ring, two measures of compression wood were derived by examining the radial series of pixels at each angular step  $r$  around an annual ring. The proportion of the ring width occupied by pixels classified as compression wood gave  $ce$ . The mean grayscale value of the pixels classified as compression wood was divided by  $T$  and then subtracted from 1 to obtain  $cc$ . Both  $cc$  and  $ce$  ranged from greater than 0 to 1, with increasing values representing more severe compression wood.

FIG. 5—Output image after equalisation of grayscale values around circumferential bands within each annual ring. Compression wood is highlighted as dark regions.



### Stem Model Construction

Given PhotoMARVL stem coordinate data and a set of disc images processed to identify annual rings and compression wood, a three-dimensional stem model was assembled as follows. In PhotoMARVL, pairs of points were digitised on the left and right edges of the stem in the approximate middle of every internode. Cardinal splines were fitted through the left and right series of points. The splines allowed interpolation of the left ( $pl$ ) and right ( $pr$ ) stem edge positions for each disc ( $d$ ) cut from the stem and were averaged to obtain the stem midpoint  $pm$ . Using compass bearings  $B1$  and  $B2$  the pair of opposing radial directions in the disc images extending left ( $rl$ ) and right ( $rr$ ) from the pith at right angles to the direction of view when the PhotoMARVL photo was taken were determined. For each disc ( $d$ ) the two over-bark radii digitised on the image ( $rr$  and  $rl$ ) were extracted and used to derive the disc midpoint  $rm$  relative to the disc image origin  $O$  at the centre of the pith. Disc data were translated into stem coordinates by first adding  $pm$  to all coordinates for the disc ( $d$ ). This located the disc origin (pith centre,  $O$ ) at the stem midpoint for that disc. Coordinates were then corrected for non-central pith by subtracting the value  $rm$  so that the disc midpoint  $rm$  coincided with the stem midpoint  $pm$ .

The splines fitted to the PhotoMARVL stem points were used to derive two measures of stem sinuosity. Tangent vectors to the splines were evaluated for each disc at  $pl$  and  $pr$ , the two vectors were averaged, and the resulting vector was normalised to unit length. The dot product of the vector with a unit length vertical vector gave a local measure of stem lean (similar to a measure used by Constant *et al.* 2003), and the projection of the vector on to a horizontal plane gave a lean direction (azimuth).

The combined data set consisted of a set of disc images, each with an associated set of points delineating pith, annual rings, and bark, all located in correct relationship to one another in three dimensions. Each point had a number of associated variables including: disc ( $d$ ), radial strip ( $r$ ), year of ring formation ( $y$ ), ring width, amount

and intensity of compression wood, stem lean magnitude and direction. Connecting points with the same  $r$  and  $y$  longitudinally and connecting points with the same  $d$  and  $y$  tangentially (taking into account continuity around the stem) formed a polygonal mesh of quadrilaterals representing the outer surface of each stem growth layer. Additionally, connecting points with the same  $d$  and  $r$  radially formed a volume composed of hexahedra, providing a three-dimensional model of the stem.

## RESULTS AND DISCUSSION

Testing of the re-mapping and smoothing process showed that  $R=720$  (0.5 degree radial steps) ensured accurate sampling of annual rings, and  $rt=4$ ,  $rr=2$  provided a useful level of smoothing, focusing more in the tangential direction (aligned with ring boundaries) than the radial direction (across ring boundaries). The output image was 720 pixels (R) by approximately 850 pixels (dependent on frame size in the original image).

The output of the re-mapping and smoothing process applied to the corrected image for disc 121/17 (Fig. 2) is shown in Fig. 3. The centre of the pith is at the top and the bark forms an undulating curve across the lower part of the image. The left edge of the image is formed from pixels along the vertical line extending upwards from the pith centre ( $O$ ) on the corrected image, and each column of pixels from left to right is sampled from successive radial strips ( $r$ ) in a clockwise direction on the corrected image. High-frequency noise was reduced by the smoothing, particularly in the tangential direction, and annual rings are now evident as approximately horizontal lines, becoming more curved at increasing distance from the pith.

The output from the oriented edge enhancement filter described earlier is shown in Fig. 4. The combination of median smoothing applied to an angular encoding of gradient values resulted in an image with high contrast. The filter parameter  $er$  allowed control over the amount of smoothing, and testing established  $er=8$  as a useful value. Positive gradient values, notably in the transition from latewood to earlywood, are evident in the output as white regions. Annual ring boundaries are represented by discontinuous white bands extending the full width of the image and there was still substantial noise, evident as scattered white pixels, present within annual rings. White bands were also generated in this image (Fig. 4) in a shaded region below the disc, but did not cause any issues during ring digitisation.

In the software implementation (program G2Ring), the image re-mapping, smoothing, and edge-enhancement processes are performed sequentially after the operator has supplied the processing parameters. These image-processing tasks typically took 4 to 5 minutes (3 to 4 minutes for re-mapping and smoothing, 1 minute or less for edge enhancement) on a Dell Latitude C810 laptop with an Intel PIII 1137MHz CPU. Because these operations were time consuming, a facility in

G2Ring was provided to batch process a list of disc images, allowing the operator to carry out other tasks.

In G2Ring an edge-detection process is applied at a location on a disc image indicated with the mouse by the user. The detection process is fast enough to allow the user to move the mouse over the image and see a resulting annual ring boundary immediately. The delineation of annual rings was carried out on the enhanced image (Fig. 4) using the edge-detection algorithm described earlier with  $ws=0.125R$  (eight segments of width 90 for  $R=720$  as used in this study) and  $rl=4$ . Thus, in the first step of the multi-scale process a curve segment of width 90 pixels is evaluated at its current location and at locations from 1 to 4 pixels above and below (in the radial sense), and if a higher value than the current location is found the curve segment is moved to that location. This is repeated for each of the eight segments to be adjusted in the first step. In successive steps the width of the segment and the height of the radial search zone are reduced until in the final step the segment width and the search height are both 1, allowing adjustment of individual pixels on the curve but only over a small distance. This multi-stage refinement process utilises more global information to approximately locate the ring in the early stages and then proceeds to refine the shape of the ring to represent local details in the later stages, respecting and utilising the important feature of ring continuity around the disc.

In this algorithm the curve shape for each new ring is based on the shape obtained for the nearest ring already delineated, beginning with a straight horizontal line for the first ring. In practice, ring detection begins at the pith-wood boundary and proceeds outwards towards the bark, reflecting the observation that inner rings are quite circular and can become more irregular with increasing distance from the pith. As a final step, the user is able to manually digitise any section of the ring boundary not delineated correctly. The digitisation process takes 5 to 10 minutes for discs such as that shown in Fig. 2. For discs with more annual rings and more irregular ring profiles the process can take up to 30 minutes. The combination of operator identification of annual rings, detailed delineation of the ring boundary by the software, and the ability of the operator to correct the boundary has proved to be an efficient method for digitising annual rings. The image of disc 121/17 from Fig. 2, with digitised annual ring boundaries superimposed, is shown in Fig. 6.

On the set of 21 discs taken at mid-internode positions along the stem of Tree 121 for this study, ring width ranged from 2.4 to 32.4 mm (average 13.5 mm) and image resolution ranged from 2.28 to 2.50 pixels/mm (average 2.42 pixels/mm). Thus, the smaller annual rings were separated by just  $2.4 \times 2.28 = 5.5$  pixels, and digitisation of these rings was at the limit of feasibility for this resolution and degree of surface noise.

Detection of compression wood was carried out on the re-mapped and smoothed disc image (Fig. 3). Use of colour information was evaluated briefly but adequate results were obtained using a grayscale image. Common problems when classifying compression wood on an image are the variations in intensity of compression wood within and between discs, and the false classification of latewood as compression wood. Compression wood is usually located in an angular sector of the disc surface, on the underside of a leaning stem in conifers. These observations led to the idea that wood in the opposite side of the stem, free from compression wood, could be used as a reference against which to compare and classify compression wood in an image. By comparing wood at equivalent positions within the same annual ring false classification of latewood as compression wood is avoided, and compression wood within the latewood can be classified using grayscale value. This approach also takes care of variations in the appearance of wood in different rings — for example, heartwood in inner rings, increasing latewood proportion in outer rings. Circumferential variations in heartwood radius, especially where heartwood has a colour distinctly different from normal wood, could cause problems with false classification as compression wood using this algorithm.

In the software implementation (G2Ring), the threshold value  $T$  is set by the operator and manual editing facilities are provided to allow for corrections. In practice, typical errors result from the false classification of patches of dirt and other contaminants on the disc surface. Annual ring boundaries and shaded regions were superimposed on an image of disc 17 (Fig. 7), indicating the proportion of ring width occupied by compression wood at each radial position (cf. Fig. 6). One issue still to be resolved is that using a single value of  $T$  to classify compression wood for the entire disc results in some over- or under-classification when the amount of compression wood varies from ring to ring.

The study carried out required a simple classification of compression wood into four classes for reporting purposes — none, mild, moderate, severe — but the image-processing algorithm was capable of discerning a much greater number of classes. As a compromise compression wood was classified into 10 classes: 0 = none, 1–9 = increasing levels of severity of compression wood. This set of 10 classes retained more information for analysis and was able to be converted to the four classes required for reporting purposes as follows: 0 none, 1–3 mild, 4–6 moderate, 7–9 severe. The values  $ce$  and  $cc$  were converted to values in the range 0 to 9,  $E$  and  $C$  respectively, as follows. Positions where compression wood was absent were assigned a value of 0. Where compression wood was present,  $ce$  and  $cc$  were mapped into the range 1–9 using Equation 1.

$$Y = 1 + \text{Round}(8x) \quad \text{Equation 1}$$

where  $Y$  represents  $E$  or  $C$  and  $x$  represents  $ce$  or  $cc$  respectively.

The software program G2Ring outputs a text data file containing the primary measurement data comprising the ring radii, the two compression wood measures ( $C$  and  $E$ ), and the two lean measures at each position  $r$  around each digitised annual ring boundary. This file is useful for further numerical processing or statistical analysis.

Given the PhotoMARVL data for a tree and a series of processed disc images, G2Ring can also output a three-dimensional stem model with associated data in the file format required for G2View. G2View is a graphical visualisation program, purpose-built for viewing two- and three-dimensional stem models with associated images and multivariate data. G2View utilises the widely used VTK software library (Schroeder *et al.* 2004) to provide underlying geometrical and graphical capabilities. G2View allows real-time interaction with the stem model, including basic facilities such as scaling, panning, and rotation of the image and allows the user to select one or more of a number of rendering options for visualising any of the data values associated with the model. In one commonly used visualisation technique, data values are mapped to a set of discrete colours. Presenting data visually is useful for discerning patterns and regions of interest — the relationships between stem shape and the location of compression wood are one example. G2View supports the simultaneous display of the disc images and a representation of the data obtained from those images blended with partial transparency. This facility is useful for comparing features of interest visible in the data with the actual appearance of the discs. A composite image depicting a number of G2View visualisation features is shown in Fig. 8.

## CONCLUSIONS

The newly developed software programs G2Ring and G2View, along with the existing PhotoMARVL system, provide a useful set of tree measurement tools. Each tool can be used on its own for specific studies and, as illustrated in this paper, they can also be used in combination to enable three-dimensional stem analysis. The ability to measure and map wood properties within tree stems is a prerequisite to understanding and modelling variation in trees. The aim is to ultimately provide knowledge and tools for applications in improved forest management, processing, and utilisation.

The main benefit of the stem analysis procedures developed is that they are image-based, avoiding the costly need to bring discs or stem sections to a laboratory from the field. Disc preparation is minimal, reducing the amount of time spent in the field, and the photographic record of disc surfaces is a useful reference and a potential data source for future studies. The visualisation tool G2View provides the means to quickly identify patterns and features of interest in the large amounts of stem data generated by the stem analysis tools described, before formal statistical analysis.

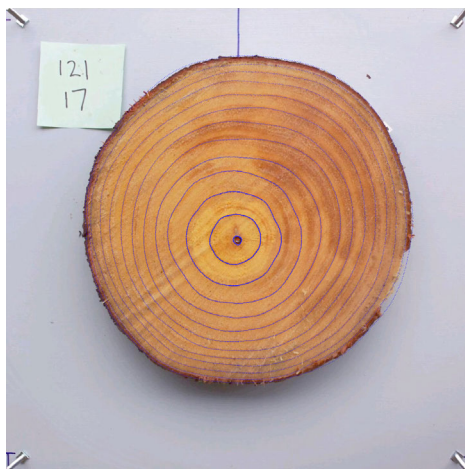


FIG. 6—Annual ring boundaries delineated on disc 121/17.

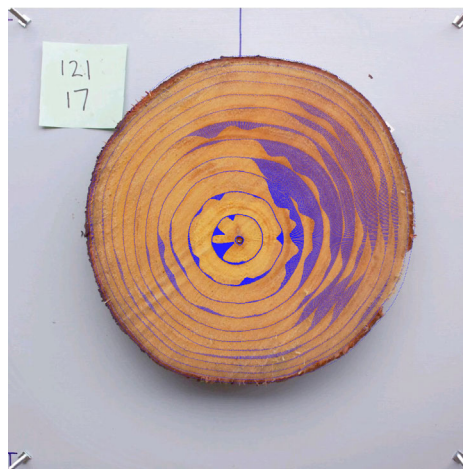


FIG. 7—Representation of compression wood ( $T=148$ ) in terms of the proportion of ring width occupied at each radial position on disc 121/17 (compare with Fig. 6).

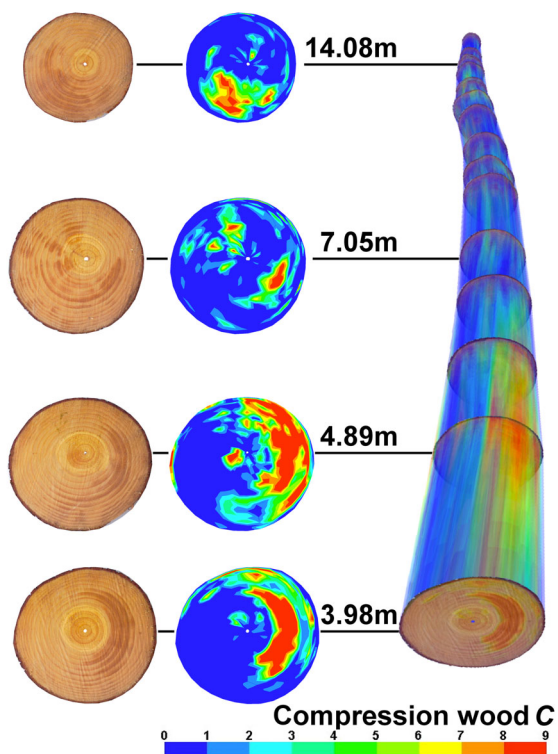


FIG. 8—Composite image of discs and 3D stem model. On the left are images of selected discs cropped to the digitised outer edge of the bark and a colour representation of the compression wood ( $C$ ) digitised for that disc. A line connects the disc images to their positions in the stem model on the right with the height of the disc in the tree given above the line.

The stem model consists of disc images and a partially transparent rendering of compression wood. Compression wood  $C$  is represented by colour according to the legend at the bottom of the figure, 0 = no compression wood, 9 = severe compression wood.

The image-processing algorithms described have been developed for use with relatively low resolution, noisy images. Improvements in disc preparation and image resolution, or use of techniques such as transmitted light through thin sections, should result in greater accuracy and improved detection of rings and compression wood from these algorithms. For discs with narrower rings this study indicated that image resolution should be chosen to provide at least 5 pixels per annual ring for the smallest annual rings. Additional surface preparation would probably also be required to allow accurate identification of ring boundaries.

The algorithms documented in this paper have been shown to provide a functional system for digitisation of annual rings and compression wood but as yet no evaluation has been made of spatial accuracy. Images were corrected for perspective distortion, leaving lens distortion as the only obvious remaining source of error in spatial accuracy inherent in the measurement system. A more significant source of error might be from operator uncertainty in identifying and locating indistinct ring boundaries. In future work a comparison should be made with radii measured by conventional means.

Future work could be usefully applied to speeding up the image re-mapping, smoothing, and ring detection algorithms as these represent the largest image-processing time components. The compression wood detection algorithm could be extended to take account of lighting variations within and between discs, possibly by the use of a reference gray sample in each image. Testing of G2Ring should be carried out to determine the spatial accuracy of digitised annual rings, the correspondence between image grayscale values and wood properties (perhaps using microscopy and SilviScan — Evans *et al.* 2001), and the repeatability of measurements. The tools described here currently provide a qualitative measure of variability in wood properties within a stem. If correlations can be found between image grayscale values and wood properties there is potential to extend the system to quantify the three-dimensional distribution of wood properties within a stem.

#### ACKNOWLEDGMENTS

The authors would like to thank Lars Hansen for suggesting the image re-mapping technique, and to acknowledge the financial support of the French Ministry of Foreign Affairs during initial development of the G2View software.

#### REFERENCES

- ALTEYRAC, J.; FOURCAUD, T.; CASTERA, P.; STOKES, A. 1999: Analysis and simulation of stem righting movements in maritime pine (*Pinus pinaster* Ait.). Pp. 105–112 in “Connection between Silviculture and Wood Quality through Modelling Approaches and Simulation Software”, Third Workshop of IUFRO, La Londe-Les-Maures, France.

- ANDERSSON, C.; WALTER, F. 1995: Classification of compression wood using digital image analysis. *Forest Products Journal* 45(11/12): 87–92.
- ASSMANN, E. 1970: “The Principles of Forest Yield Study. Studies in the Organic Production, Structure, Increment and Yield of Forest Stands”. Pergamon Press, Oxford.
- BIGING, G.S.; WENSEL, L.C. 1984: A photographic technique for use with stem analysis. *Forest Science* 30(3): 715–729.
- BURDON, R. 1975: Compression wood in *Pinus radiata* clones on four different sites. *New Zealand Journal of Forestry Science* 5: 152–164.
- CONNOR, W.S. 1999: A computer vision based tree ring analysis and dating system. M.Sc. thesis, The University of Arizona.
- CONSTANT, T.; MOTHE, F.; BADIA, M.A.; SAINT-ANDRE, L. 2003: How to relate the standing tree shape to internal wood characteristics: Proposal of an experimental method applied to poplar trees. *Annals of Forest Science* 60: 371–378.
- DUFF, G.H.; NOLAN, N.J. 1953: Growth and morphogenesis in the Canadian forest species. I. The controls of cambial and apical activity in *Pinus resinosa* Ait. *Canadian Journal of Botany* 31: 471–513.
- 1957: Growth and morphogenesis in the Canadian forest species. II. Specific increments and their relation to the quantity and activity of growth in *Pinus resinosa* Ait. *Canadian Journal of Botany* 35: 527–572.
- DUNCKER, P.; WARENSJÖ, M. 2005: Compression wood: literature review [Online]. Available: <http://www.forestry.gov.uk/website/forestresearch.nsf/ByUnique/GGAE-5GGEAX> [November 2005].
- EVANS, R.; KIBBLEWHITE, R.P.; STRINGER, S.L. 2001: Variation in microfibril angle, density and fibre orientation in twenty-nine *Eucalyptus nitens* trees. *Appita Journal* 53(5): 450–457.
- FIRTH, J.G.; BROWNLIE, R.K.; CARSON, W.W. 2000: Accurate stem measurements: key to new image-based system. *New Zealand Journal of Forestry* 45(2): 25–29.
- GUAY, R.; GAGNON, R.; MORIN, H. 1992: A new automatic and interactive tree-ring measurement system based on a line scan camera. *Forestry Chronicle* 68: 138–141.
- HARRIS, J.M. 1976: Shrinkage and density of radiata pine compression wood in relation to its anatomy and mode of formation. *New Zealand Journal of Forestry Science* 7(1): 91–106.
- HARRIS, J.M.; COWN, D.J. 1991: Basic wood properties. Pp. 6-1 – 6-28 in Kininmonth, J.A.; Whitehouse, L.J. (Ed.) “Properties and Uses of New Zealand Radiata Pine Vol. 1. Wood Properties”. Forest Research Institute, Rotorua.
- HUSCH, B.; BEERS, T.W.; KERSHAW, J.A. 2003: “Forest Mensuration”. Fourth edition. John Wiley & Sons Inc., Hoboken, New Jersey.
- NICHOLLS, J. 1982: Wind action, leaning trees and compression wood in *Pinus radiata*. D Don. *Australian Forest Research* 12: 75–91
- NYSTRÖM, J.; KLINE, D.E. 2000: Automatic classification of compression wood in green southern yellow pine. *Wood and Fiber Science* 32(3): 301–310.
- PILLOW, M.Y. 1941: A new method for detecting compression wood. *Journal of Forestry* 39: 385–387.

- SAINT ANDRÉ, L.; LEBAN, J.M. 2000: An elliptical model for tree ring shape in transverse section. Methodology and case study on Norway Spruce. *Holz als Roh-und Werkstoff* 58: 368–374.
- SCHROEDER, W.; MARTIN, K.; LORENSON, B. 2004: “The Visualization Toolkit: An Object-oriented Approach to 3D Graphics”. Third edition. Kitware Inc.
- SOILLE, P.; MISSON, L. 2001: Tree ring area measurements using morphological image analysis. *Canadian Journal of Forest Research* 31: 1074–1083.
- TIMELL T.E. 1986: “Compression Wood in Gymnosperms” Vol. 1. Springer, Berlin.
- WARENSJÖ, M.; NYLINDER, M.; WALTER, F. 2004: Modelling compression wood using data from a 3D-laser scanner. Pp. 178–185 in Nepveu, G. (Ed.) Proceedings of the IUFRO WP S5.01.04 Fourth workshop “Connection between Forest Resources and Wood Quality: Modelling Approaches and Simulation Software”, Harrison Hot Springs, British Columbia, Canada, 8–15 September 2002.
- WERNSDÖRFER, H.; RECK, P.; SEELING, U.; BECKER, G.; SEIFERT, T. 2004: Erkennung und messung des reaktionsholzes bei fichte (*Picea abies* (L.) Karst.) mittels verfahren der digitalen bildanalyse. *Holz als Roh-und Werkstoff* 62: 243–252.
- WinDENDRO 2004: “WinDENDRO Reference Manual”, V 2004a, August. Regent Instruments, Quebec.
- WOLF, P.R. 1983: “Elements of Photogrammetry”. Second edition. McGraw-Hill, Singapore.
- YANOSKY, T.M.; ROBINOVE, C.J. 1986: Digital image measurement of the area and anatomical structure of tree rings. *Canadian Journal of Botany* 64: 2896–2902.